Journal of Radioanalytical and Nuclear Chemistry (2021) 328:1085–1098
https://doi.org/10.1007/s10967-021-07708-w

Aggrandizement of uranium (VI) removal performance of *Lentinus concinnus* biomass by attachment of 2,5-diaminobenzenesulfonic acid ligand

Omur Celikbıcak[1] · Gulay Bayramoglu[2,3] · Ilkay Acıkgoz-Erkaya[4] · Mehmet Yakup Arica[2]

Received: 11 January 2021 / Accepted: 1 April 2021 / Published online: 27 April 2021

Abstract
In this study, the native and 2,5-diaminobenzene sulfonic acid (DABSA) attached *Lentinus concinnus* biomasses were utilized for removal of U(VI) ions from solutions. At 25 °C, the maximum uranium ion adsorption capacity of the native and DABSA attached fungal biomasses were found to be 118.6 and 539.2 mg/g, respectively, at pH 6.0. The negative ΔG° values of U(VI) removal showed that the adsorption procedure were spontaneous. ATR-FTIR data showed that U(VI) ions adsorption the adsorbents was mainly attributed by amine, carboxyl and sulfate groups.

Keywords *Lentinus concinnus* · Fungal biomass · Sulfate functionalization · U(VI) removal · Thermodynamic parameters

Introduction

One of the common radionuclide pollutants, especially uranium (U), arises from the production of nuclear fuel released into the ecological environment [1–4]. For the safe development of the nuclear industry, the disposal of nuclear waste is very important due to the long half-life of uranium. Uranium is also considered to be dangerous radioactive contaminant [5–9]. It should be noted that the normal activity of the kidney, brain, liver, heart, and reproductive system could be destroyed by uranium exposure. The storage and collection of a waste radioactive substance in a large amount in the environment can menace human health and consequently cause to various diseases and carcinogenesis [10, 11]. Until today, for U(VI) removal from aqueous media, many physical, chemical and biological treatment processes have been investigated [12–16]. These researches have been placed in scientific publications with all advantages and disadvantages [17–19]. It is known that, these earlier reports will help the solution of further ecological problems with each passing day developing and innovating technologies. Many methods have been developed removal of radionuclides from the aqueous medium such as adsorption, coagulation, reverse osmosis and solvent extraction [20–25]. The adsorption method is low rate and environmentally applicable technique, and various adsorbents have used such as activated carbon, clay mineral, ion-exchange resins and biosorbents applied to remove radionuclides [26–30]. Besides, many natural microbial biomass and their derivatives, and natural polymers (such as alginate, agarose, and cellulose) have been utilized for removal of various metals and radioactive elements from the environment [27]. Living or nonliving microbial and plant biomasses can be favorable adsorbents for the removal of metals from aqueous medium [31–35]. Moreover, the alteration of the adsorbent surface with useful groups could improve the adsorbent performance and adsorption capacity. Different microbial biomasses such as fungi, algae, and bacteria have been functionalized with ion-exchange ligands for the development of a more effective sorbent [28, 32]. Fungal biomasses have been demonstrated to be cost-effective materials, as fungi plentifully cultivated in natural environments [28, 36]. Furthermore, fungal biomasses have a high metal ion adsorption performance due

✉ Gulay Bayramoglu
g_bayramoglu@hotmail.com

1 Department of Chemistry, Faculty of Sciences, Hacettepe University, 06800 Beytepe, Ankara, Turkey

2 Biochemical Processing and Biomaterial Research Laboratory, Faculty of Science, Gazi University, 06500 Teknikokullar, Ankara, Turkey

3 Department of Chemistry, Faculty of Sciences, Gazi University, 06500 Teknikokullar, Ankara, Turkey

4 Department of Environmental Science, Faculty of Engineering and Architecture, Ahi Evran University, Kırşehir, Turkey

to the presence of high quantities of polysaccharides, proteins, and many kinds of organic acids (such as teichoic and teichuronic acid on the fungal cell walls. The surfaces of fungal cells have numerous amounts of useful groups (such as $–NH_2$, –OH, –COOH, $–HPO_4$, and $–HSO_3$) those can show as adsorptive sites for metals [28]. Especially, white-rot fungi have large surface areas due their mycelial structures [28].

In this work, *Lentinus concinnus* (*L. concinnus*) biomass was modified with DABSA ligand. It has two pKa values, and one is acidic and the other one is basic, therefore, it is a Zwitterionic ligand. Adsorption of uranium (VI) from aqueous solution was studied using the native and the DABSA attached *L. concinnus* biomass. The properties of fungal preparations were investigated by Fourier transformed infrared spectroscopy (FTIR), scanning electron microscope (SEM), Brunauer–Emmett–Teller (BET) method and zeta seizer. The surface zeta potentials could provide information about the ionization of adsorptive groups upon changes in the pH. *L. concinnus* is a white rot fungus and possesses good pollutants removal ability due to the presence of numerous functional groups on its hyphae surfaces, and has not been used previously for U(VI) ion adsorption. This is the first report to control the adsorption efficacy of DABSA ligand-attached *L. concinnus* biomasses.

Experimental

Materials

U(VI) solution was prepared by dissolving uranyl acetate ($UO_2(CH_3COO)_2{\cdot}2H_2O$; acetate salt of uranium) in purified water and obtained from Honeywell Riedel-de-Haën AG (Germany). Chloroacetic acid, NaOH, arsenazo(III) (1,8-dihydroxynaphthalene-3,6-disulfonic acid-2,7-bis[(azo-2)-phenylarsonic acid), HCl, glutaraldehyde, glycerol, diiodamethane and 2,5-Diaminobenzenesulfonic acid (DABSA) were obtained from Sigma-Aldrich. The color developing reagent was prepared by dissolving of arsenazo(III) (0.5 g/L) in purified water. The sodium chloroacetic acid–sodium acetate buffer was prepared by dissolving of chloroacetic acid (200 g) and sodium hydroxide (40 g) in purified water (300 mL). Then, the mixture was added in a volumetric flask (1.0 L) and completed to 1.0 L with purified water.

Cultivation and Modification of *L. concinnus* biomass with DABSA ligand

The white rot fungus *L. concinnus* strain MAFF 430,305 was obtained from the National Institute of Agrobiological Sciences (NIAS), Tsukuba, Ibaraki, Japan. The fungus was cultivated in Sabouraud Dextrose Broth medium using the shake flask method as described previously [28]. The biomass of *L. concinnus* (approximately 2.0 g) was transferred in Tris–HCl buffer (100 mL, 50 mM, pH 8.0) and glutaraldehyde (GA) solution (50 mL, 1.0%) and the surface of the fungal biomass was functionalized at 45 °C for 6.0 h while continuously shaking in a water bath. Subsequently, the GA activated *L. concinnus* biomasses (approximately 2.0 g) were added ethanol/water mixture (70:30, v/v ratio, 200 mL) containing DABSA ligand (20 mg/mL), and the modification reaction was carried out at 25 °C for 8.0 h. The DABSA ligand attached fungal biomass was washed with Tris–HCl buffer (50 mM, pH 7.0). They were dried under reduced pressure at 40 °C for 12 h. The modification protocol of the *L. concinnus* biomass with DABSA ligand is presented in Fig. 1. The weight gain (WG) was calculated by using percent increase in weight of the fungal biomass:

$$\mathrm{WG}(\%) = \left(\mathrm{W_g} - \mathrm{W_i}\right)/\mathrm{W_i} \times 100 \quad (1)$$

where W_i and W_f are the weights of the fungal biomass before and after modifications with DAPSA ligand, respectively.

Adsorption studies of uranium (VI)

The removal of U(VI) ions using the native and DABSA attached *L. concinnus* biomasses was studied using a batch system. Uranium solutions with different amounts were prepared from a stock solution (1000 mg/L in purified water). Adsorption studies were carried out using fungal biomass (10 mg) in 25 mL of uranyl ions solution (200 mg U(VI)/L) at 25 °C for 2.0 h. The effect of pH and ionic strength on the U(VI) adsorption was realized in the pH range 2.0 to 8.0 and at different NaCl concentration between 0.1 and 1.0 mol L^{-1}, respectively. The effect of adsorbent dosage on the adsorption performance was performed by varying fungal biomass in the medium between (0.1 and 1.0 g/L) in the medium. The effect of temperature was realized at varying temperatures (i.e., 15, 25 and 35 °C). The effect of initial concentration of uranium on the adsorption efficacy was evaluated by changing the concentration of U(VI) ions between 25 and 500 mg/L. The arsenazo(III) method was used for determination of U(VI) samples in the medium as described earlier [37]. The U(VI) concentration in the medium was determined using a double beam UV/vis spectrophotometer (PG Instrument Ltd., Model T80 + ; PRC) at 651 nm. A calibration curve for U(VI) was obtained by plotting absorbance (A651) versus U(VI) ions. The amount of U(VI) ion adsorbed per unit of fungal biomass sample (mg U(VI)) ions per gram dry fungal biomass) was calculated as reported earlier [28].

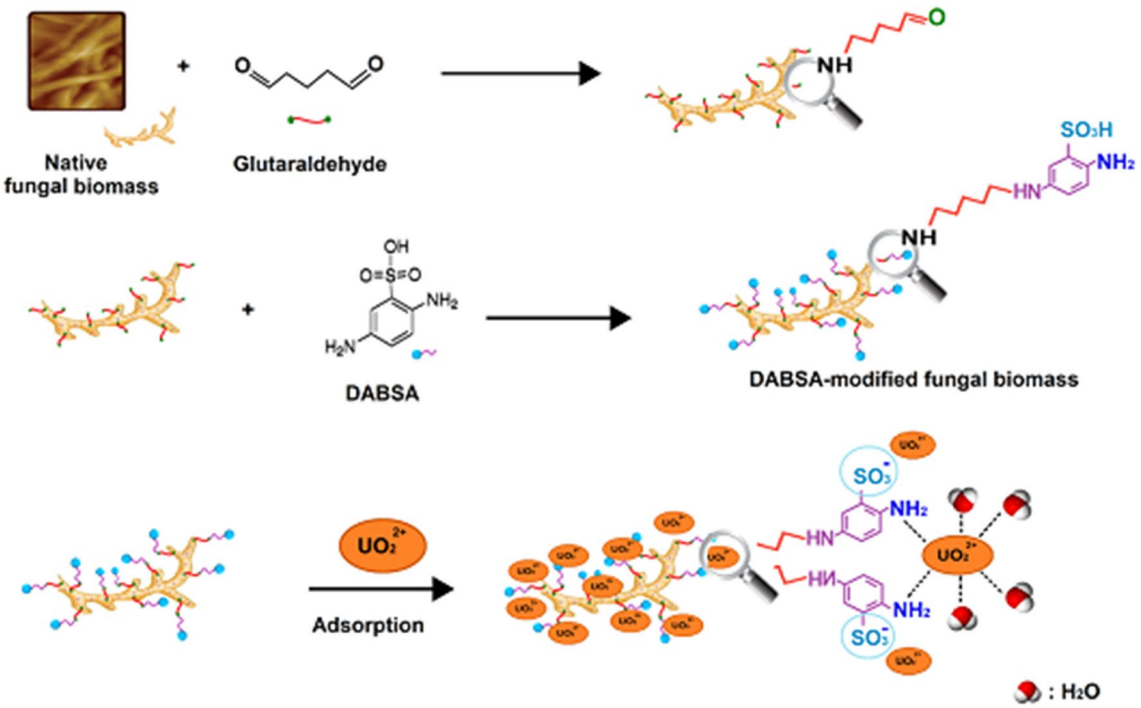

Fig. 1 Modification protocol and chemistry of the DABSA modified fungal biomass

Reusability studies of the adsorbents

Reusability of adsorbents were tested five times using the same fungal biomass samples. Desorption of U(VI) ions was studied by using HNO_3 solution (10 mmol/L). The uranium adsorbed fungal biomass was added in desorption medium and magnetically stirred at 100 rpm for 2.0 h at room temperature. After adsorption–desorption sequence, the fungal biomass sample was washed with NaCl (0.1 mol/L) solution. Then, it was transferred into a new medium containing uranyl ion for the next round.

Characterization of the native and DABSA-ligand attached fungal biomasses

ATR-FTIR spectra of the native and DAPSA ligand attached fungal biomasses were obtained by using an attenuated total reflectance Fourier-transform infrared (ATR-FTIR) spectrometer (Nicolet IS 5, Thermo Electron Scientific Instruments, WI, USA). The surface areas and pore volume of the fungal biomass preparations were obtained by using the Brunauer, Emmett and Teller (BET) method. The contact angle values of the native and DAPSA ligand attached fungal biomass were studied using three test liquids namely water, glycerol and diiodomethane). Digital optical contact angle meter were used for determination of contact angle values of the materials (Phoenix 150, Surface Electro Optics, Korea). The amounts of total sulfate groups of the DAPSA ligand attached fungal biomass samples were determined by a method as described previously [38]. Briefly, the sulfate groups of the DABSA modified fungal biomass were determined by potensiometric titration. The sulfate modified biomass (about 0.1 g) were added into NaOH solution (0.2 mol/L, 10.0 mL) and the solution was incubated in a shaking water-bath at 35 °C for 4.0 h. Then, the final concentration of NaOH in the solution was determined with titration of 0.05 mol/L HCl solution. The zeta potential measurement was studied with a Zeta-sizer (NanoZS, Malvern Instruments Ltd., Malvern, UK) as described earlier [32].

Results and discussion

Properties of the *L. concinnus* biomass preparations

In this study, native and DABSA ligand attached *L. concinnus* biomasses were prepared and used for removal of U(VI) ions from aqueous solutions. *L. concinnus* is a wood-decaying fungus and cultivates on the abundant carbon source "cellulose". The main components of the cell walls of fungi are glucans, lipids and proteins. The fungal cell wall proteins have several pendant amino acids residues, such as amine, thiol and carboxyl groups. The lysine and arginine residues of proteins donate pendant amine groups for reaction of bifunctional aldehyde linker. Thus, these functional groups of the fungal biomass can be easily reacted with

glutaraldehyde for further modification. The addition of DABSA ligand on *L. concinnus* biomasses supplied additional binding sites for adsorption of U(VI) ions (Fig. 1). The BET studies showed that of the native and DAPSA ligand attached *L. concinnus* biomasses have moderately low specific surface area. The specific surface area was obtained as 0.524 and 0.476 m^2 for the native and DAPSA ligand attached biomasses, respectively. The modification process did not significantly affected of the surface properties of the fungal biomass. The specific surface areas of the fungal preparations were in the same order of magnitude. This result showed that the fungal biomasses preparations could not be considered very porous adsorbent, and additionally, the surface area of the DAPSA ligand attached fungal biomass was reduced about 10.5% compared to native biomass. After modification with DAPSA ligand, the increase in the weight of the fungal biomass was found to be 71.6%.

To determine the presence of functional adsorption groups (i.e., hydroxyl, amine, carboxyl and sulfate) on both the native and DAPSA ligand attached fungal biomasses, The ATR-FTIR spectra of the native and DAPSA ligand attached *L. concinnus* were obtained. The results are presented in Fig. 2. Generally, the native fungal biomass has peaks at 3274 and 1540 cm^{-1} representing amino groups stretching vibrations (Fig. 2A). The hydroxyl groups of water and polysaccharides stretching vibrations peaks of the fungal biomass preparations should be superimposed on the amine groups peaks at 3274 cm^{-1}. The band at 2920 cm^{-1} can be recognized as C-H broadening. The peaks at 1629, 1375 and 1201 cm^{-1} are due to the carbon double bond oxygen stretching peaks of carbonyl groups. The peak at 1032 cm^{-1} exhibits of the characteristic C-O stretching vibrations in amine and alcohol groups on the native fungal biomasses. After modification of fungal biomass with DABSA ligand, the spectrum of the DAPSA ligand attached fungal biomass displayed some variations (Fig. 2B). The peaks at around 3300 cm^{-1} are broadened, it could be due to the incorporation of a large number of amine groups via the DABSA ligand. Moreover, the peak at 2920 cm^{-1} is shifted to 2855 cm^{-1}. The FTIR spectrum for DAPSA ligand attached fungal biomass displays that the peaks produced by C–C and C–N stretching vibrations moved to higher wave number values of 1573 and 1484 cm^{-1}, respectively, afterward attachment of DABSA ligands. Additionally, the new bands at 1413 and 929 cm^{-1} are representative of the S=O stretching vibrations of sulfonic acid group on the DABSA ligand. The observed other new bands at 1151 and 1025 cm^{-1} can characterize as asymmetric and symmetric S=O stretching vibrations, respectively, from the sulfonate group on the DABSA ligand. This observation indicated that the attachment of DABSA ligand was successful on the fungal biomass using glutaraldehyde bifunctional agent. Additionally, in the ATR-FTIR spectrum of the DAPSA ligand attached fungal biomass the peaks at 1545 and 1719 cm^{-1} were not observable, whereas additional peaks were observed as indicated above.

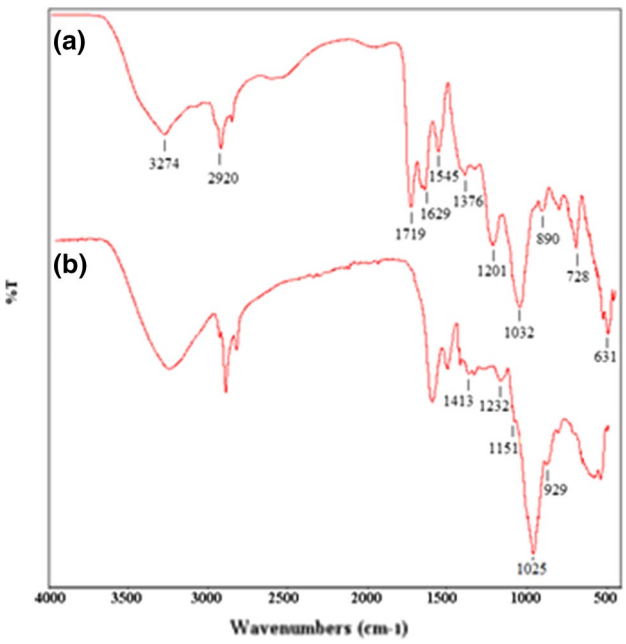

Fig. 2 FTIR spectra: the native (**a**) and DABSA modified (**b**) fungal biomass preparations

The contact angle data of the native and DABSA ligand attached and their U(VI) contacted counterpart's samples were obtained by using three different test liquids (i.e., water, glycerol, and diiodomethane). All the tested *L. concinnus* biomasses showed dissimilar contact angle values according to the surface properties (Table 1). The water contact angle value of the native fungal biomass was 106.8 ± 2.3. Thus, it has a hydrophobic surface. Whereas the water contact angle value of the DAPSA ligand attached fungal biomass was decreased, this could be due to the incorporation of a secondary, primary and sulfate group via attachment of DABSA ligand. Thus, the hydrophilicity of the DAPSA ligand attached fungal biomass was considerably enhanced

Table 1 Contact angle data for water, glycerol and diiodamethane for the native, and DABSA modified fungal biomass preparations

Fungal biomass	Water, θ (°) (γ erg = 71.3)	Glycerol, θ (°) (γ erg = 64.0)	DIM, θ (°) (γ erg = 50.8)
Native	106.8 ± 2.3	93.7 ± 2.1	54.1 ± 1.8
Native-U(VI)	69.8 ± 2.5	79.1 ± 2.3	41.1 ± 1.5
DABSA-modified	58.1 ± 1.3	51.3 ± 2.2	32.3 ± 1.1
DABSA-Modified-U(VI)	63.7 ± 3.2	75.8 ± 2.7	36.3 ± 1.2

γ erg: surface tension of test liquid

compared to native one. These functional groups are notably important for adsorption of U(VI) ions. The wettability of a newly designed sorbent could be estimated by comparing the contact angle data of water and diiodomethane. Since, these two liquids are frequently used for reference fluids in investigation of the hydrophilic or hydrophobic properties of the adsorbent. After U(VI) adsorption the contact angle values of both adsorbents were significantly altered due to the interaction of uranyl ions with the fungal biomass preparations. This could be prepotency of hydrophobic entities of U(VI) ions on the fungal biomass surfaces.

The SEM micrograph of the native *L. concinus* mycelia is presented in Fig. 3. As observed from the SEM images, that there are several hyphae on the rough surface of the fungal biomass (Fig. 3A). Thus, these hyphae structures enhance the surface area of the fungal biomass and promising the removal performance for the uranium ions. It should be noted that the observed alteration of surface morphology of *L. concinus* mycelia is unimportant after modification with DABSA ligand (Fig. 3B).

Effect of adsorbent dosage on the U(VI) removal efficacy

The adsorbent dosage is one of the significant parameter that controls the removal process of U(VI) ions from the solution. The native and DAPSA ligand attached fungal biomasses were tested for their U(VI) removal efficiency from aqueous solution. Figure 4 displays the relationship between the U(VI) removal efficiency of and the amount of algal biomass preparation in the adsorption medium. As can be seen from the figure, by increasing both fungal biomass dosage from 0.1 to 0.4 g/L, the U(VI) removal

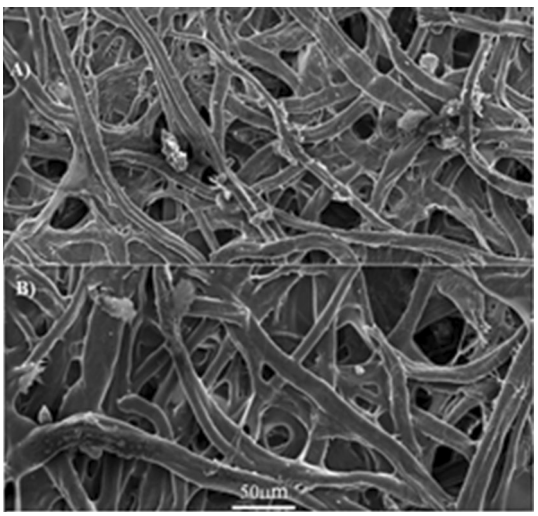

Fig. 3 SEM micrograph of the fungal biomass preparations: the native (**A**) and DABSA modified (**B**) fungal biomass preparations

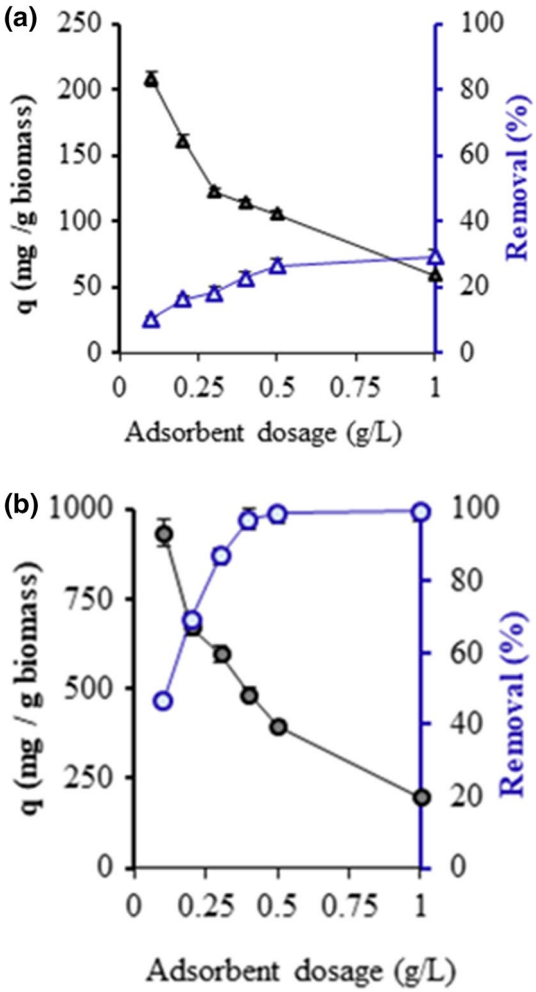

Fig. 4 Effect of the native (**a**), and DABSA modified (**b**) fungal biomass preparations dosage on the adsorption performance of U(VI)

percentage of both the native and DAPSA ligand attached fungal biomasses increased. This could be due to increase the available adsorptive sites on both fungal biomass preparations which could interact to U(VI) ions in the medium [39–41]. Whereas the fungal biomasses dosage increases from 0.5 g to 1.0 g/L, the adsorption capacities of both the tested biomasses continue to reduce. This could be due to the available adsorptive site of the tested fungal biomasses had not reached to full saturation when adsorption process became equilibrium. For this reason, the removal efficiencies of both adsorbents continuously increased as the amount of adsorbent increased in the adsorption medium. As presented in Fig. 4, after each the fungal biomass dose reaching to 0.4 g/L, there was no substantial change of adsorbent on U(VI) adsorption rate. Therefore, 0.4 g/L of fungal biomass was designated for the remaining adsorption experiment.

Effect of pH on U(VI) adsorption and Zeta potential measurements

The effects of the medium pH on the adsorption capacities of the native and DABSA ligand attached fungal biomasses were examined in the pH range 2.0–8.0 at 25 °C. For the adsorption of U(VI) ions on adsorbents, the most important factor is the ionization state of the functional groups of the used materials, and the pH of the medium is an essential parameter for the functional chemical groups on the surface of adsorbent. Therefore, the adsorption capacities of the native and DABSA ligand attached fungal biomasses are determined by the ionization state of the surface functional groups and the speciation of U(VI) ions in the aqueous medium. The attached DABSA ligand has a steady negative charge due to presence of strong acidic sulfonate groups in the studied pH range, and it is not hardly influence by the change in the pH of the medium. Therefore, the DABSA ligand attached fungal biomass could have an adsorption capacity at the tested pH ranges due to the present of the strong sulfonic acid groups. As observed from Fig. 5, the maximum amounts of U(VI) adsorption on the native and DABSA ligand attached fungal biomasses were found to be at pH 6.0 and 5.0, respectively. Further increase or decrease in these pH values was found to be decrease the adsorption capacities of both the tested adsorbents. The higher U(VI) removal efficiencies at between pH 5.0 and 6.0 for the fungal biomass preparation could be ascribed to the surface properties of the native and DABSA ligand attached fungal biomass preparations. Thus, the effect of pH on the fungal biomasses could be described in terms of the electrostatic interactions introduced by the functional groups of the tested adsorbents [45–47]. The detected lesser adsorption performance at low pH values could be due to the existence of high H + ions concentrations. From Fig. 5, the adsorption capacities of native and DABSA ligand attached fungal biomasses to U(VI) ions steeply improved with the increase of the solution pH from 2.0 to 6.0 and 2.0 to 5.0, and reduced with more increasing of the medium pH from 6.0 to 8.0 for both tested adsorbents, respectively. Thus, the maximum adsorption capacities of native and DABSA ligand attached fungal biomasses were found to be 113.8 mg/g at pH 6.0 and 485.4 mg/g at pH 5.0 for 200 mg L^{-1} U(VI) concentration, respectively. The observed high removal efficacy for DABSA ligand attached fungal biomass should be due to the presence of two amino groups and a sulfate groups due to the attachment of DABSA ligand. At low pH values, the opposition is larger between H^+ from the solution and the U(VI) ions and they compete with each other for the functional binding sites. At between pH 5.0 and 6.0, the major uranium species occur in the solution as $[(UO_2)_2(OH)_2(II)]$, $[(UO_2)_4(OH)(VII)]$, $[(UO_2)_4(OH)_6(II)]$, and $[(UO_2)_4(OH)_2(VI)]$. Thus, the maximum capacities could be increased due to the reducing of the amount of protonation. When the solution pH above 6.0, U(VI) ions can be easily hydrolyzed into carbonate species (i.e., $(UO_2)_2(CO_3)(OH)_3$ from pH 6.0 to 8.0 [28, 42–44]. This can cause reduction in the adsorption capacities of the adsorbents. These results show that the native and DABSA ligand attached fungal biomasses had the maximum adsorption capacity at pH 6.0 and 5.0, respectively. Thus, these pH values were used in the remaining studies.

Zeta potential measurement can give evidence about the surface charge properties of the materials. The zeta potential value of a material relies on the density of its negative or positive charges, and the solution pH. The pH values at the point of zero charge for the native and DAPSA ligand attached fungal biomasses were obtained as approximately 3.8 and 4.5, respectively, from the plot of zeta potential (mV) against pH (Fig. 6). As can be seen from the figure, the DAPSA ligand attached fungal biomass had more negatively

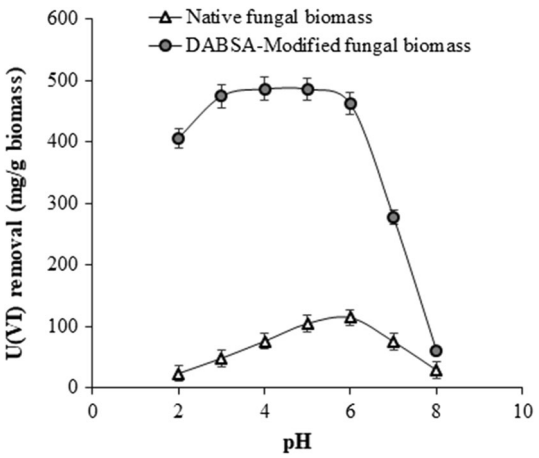

Fig. 5 Effect of pH on U(VI) ions adsorption on the native, and DABSA modified fungal biomass preparations

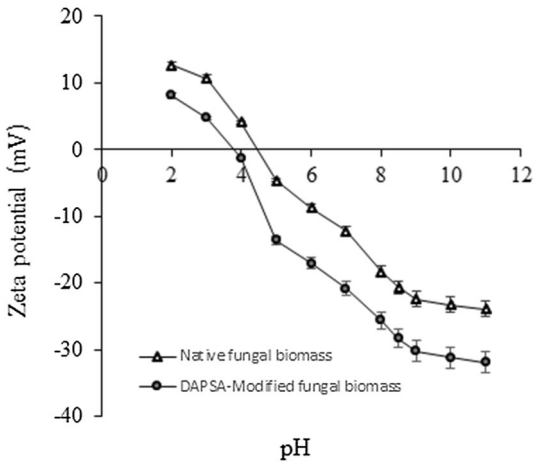

Fig. 6 pH versus zeta potential plots for the native and DABSA modified fungal biomass preparations

charged than the native counterpart. The charge densities in the studied pH ranges have altered from – 23.9 to 12.6 mV for the native fungal biomass and – 31.9 and 8.1 mV for the DAPSA ligand attached fungal biomass. The native fungal biomass has the highest positive zeta potential value (12.6) compared to DAPSA ligand attached biomass (8.1). It should be noted that the native fungal biomass surface composed of the various functional groups (such as hydroxyl, carboxyl, sulfhydryl, imidazole, phosphate, amine and amide). On the other hand, DAPSA ligand attached fungal biomass has additional an aromatic ring with two amine and sulfonate groups. As observed from the figure, the shape of the zeta potential curves of both the adsorbents surfaces had amphoteric characteristic. These functional groups on the fungal based adsorbents surfaces are protonated or deprotonated according to the medium pH, and the overall surface net charge densities are zero at the point of zero charge. The DAPSA ligand attached fungal biomass has a good adsorption capacity approximately 485.4 mg/g at pH 5.0 which is higher most of the recognized ion-exchange adsorbents. It should be noted that the sulfonate groups of the DAPSA ligand attached fungal biomass have adequately low pKa values to persist completely charged over the working pH range. The modification of fungal biomass with zwitterion ligand (i.e., DABSA) could elucidate the preparation of high capacity adsorbent with application in the removal of metals from aqueous medium.

Effect of ionic strength on adsorption performance of the adsorbents

The effect of ionic strength was realized by varying ionic strengths (NaCl concentrations from 0 to 1.0 mol/L). As observed from Fig. 7, the effect of NaCl concentration on the adsorption of U(VI) ions on both adsorbents was not substantial when the concentration of NaCl was low. As the NaCl concentration was enlarged, the U(VI) ions adsorption decreased progressively for both tested adsorbents. This reduction of the adsorption capacity of the adsorbent upon increasing NaCl concentration could be probably due to a higher interaction of binding sites with the electrolytes. The adsorption capacities of the adsorbents in the NaCl free U(VI) solution were found to be 113.8 and 485.4 mg/g, respectively. At 1.0 mol/L NaCl concentration, the adsorption capacities were obtained as 37.3 and 169.1 mg/g for native and DAPSA ligand attached fungal biomasses, respectively. The negative and positive charges on the adsorbents are screened by the opposite charges of the electrolytes (i.e. Na^+ and Cl^-). Thus, the thickness of the double layer could determine the binding performance of the target metal ions on the functional groups of the adsorbents. An addition, the increase in medium ionic strength can have managed to the construction of ions pairs between uranyl ions and

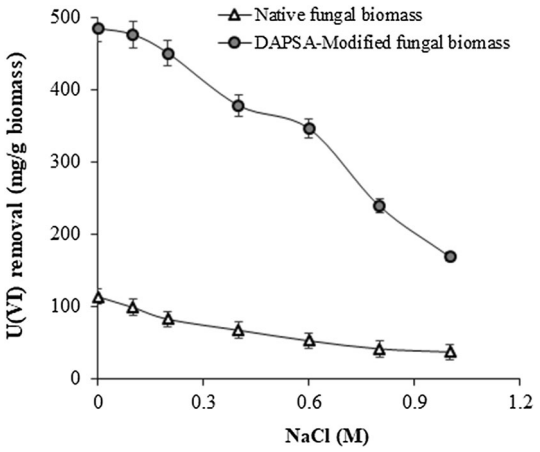

Fig. 7 Effect of ionic strength on U(VI) ions adsorption on the on the native, and DABSA modified fungal biomass preparations

anions (Cl^-) present in the solution and thus, reduced the activity of the free uranyl ions in the solution for binding sites. Moreover, obtained results affirmed that the native and DAPSA modified fungal biomass can be influenced by varying the ionic strength of the solutions which affect the electrostatic forces of the fixed charges of the adsorbents (i.e., $–NH_3^+$ and $–SO_3^-$). The DAPSA modified fungal biomass was more sensitive to ionic strength compared to native fungal biomass. At 0.1 mol/L salt concentration, the native and DAPSA modified fungal biomass were not responsive to Na^+ and Cl^- ions while at 1.0 mol/L, a high binding inhibition effect was observed for both Na^+ and Cl^- ions pairs in the system. This was more pronounced for the DAPSA modified biomass than that of the native counterpart. This is due to presence of net positive ($–NH_3^+$) and negative charges ($–SO_3^-$) on the modified fungal biomass.

Effect of initial U(VI) ions concentration and isotherm studies

The effect of the initial concentration of U(VI) ions on the removal efficiency of the native and DAPSA ligand attached fungal biomasses was realized at concentrations between 25 and 500 mg/L, and at three different temperatures. As observed from Fig. 8, the adsorption capacities of both native and DAPSA attached fungal biomasses increased with increase in the initial U(VI) concentration in the medium. At low uranyl ions concentrations, the adsorption capacity rapidly enhanced and then reached plateau values of 118.6 and 539.2 mg/g at an initial concentration of 400 mg/L. This could be due to the generated concentration gradient is small, thus, the diffusion coefficient or mass transfer coefficient is reduced consequently causes a slower transport of ions from bulk to adsorbent surfaces. When the initial concentration of metal ions in

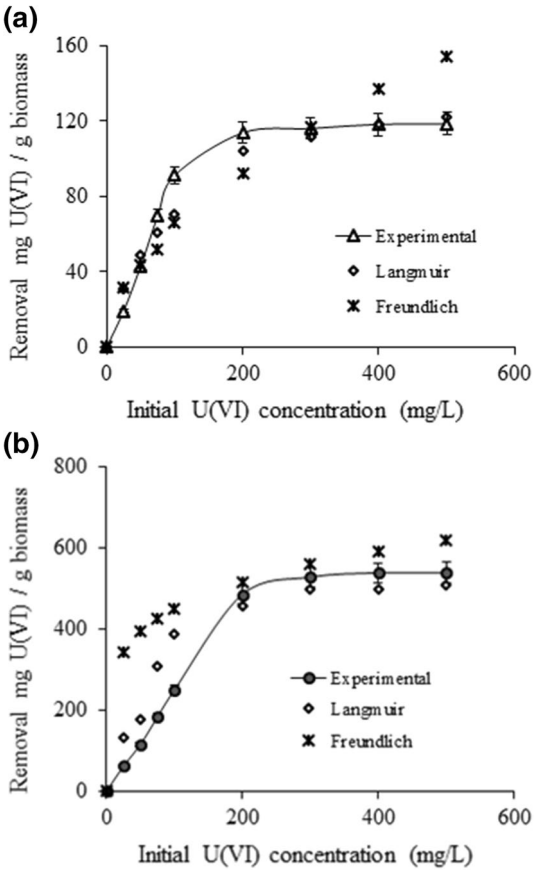

Fig. 8 Effect of initial concentration of U(VI) ions on adsorption of the native, and DABSA modified fungal biomass preparations

the solution is enlarged, the dynamic force for mass transfer from bulk to adsorbent also increases [48–50]. To evaluate U(VI) ions adsorption mechanism and to analyze the experimental adsorption data, the Langmuir and Freundlich models are tested to fit the experimental equilibrium adsorption data. These isotherm models equations are:

$$q = \left(q_{max} b C_{eq}\right) / \left(1 + b C_{eq}\right) \quad (2)$$

$$q = KF\left(C_{eq}\right)^{1/n} \quad (3)$$

The Langmuir and Freundlich isotherm parameters were calculated from the intercept and slope of the plots of isotherm models. The isotherm plots and parameters are presented in presented in Fig. 8 and Table 2. From the table, the theoretical adsorption capacities were over approximately 14% for native fungal biomass and 1.8% for DAPSA ligand attached fungal biomass at 25 °C. As can be seen from Fig. 8, the Langmuir model fitted the experimental data for both fungal biomass preparations. The Langmuir model gave high correlation coefficients (R^2) for both adsorbents, which confirmed that the Langmuir model could appropriately define the experimental adsorption data. The values of RL show the shape of the Langmuir isotherm model: unfavorable adsorption (RL > 1), linear adsorption (RL = 1), promising adsorption (0 < RL < 1), or irreversible adsorption (RL = 0) [28, 32]. The obtained RL values for both tested adsorbents are presented in Table 2. The RL values were between 0 and 1, which showed that the adsorption of U(VI) ion from aqueous medium by fungal biomass preparations was favorable. For the Freundlich isotherm models, the degree of KF and n values of Freundlich model displayed easy removal of U(VI) ions from solutions. Values of n are greater than 1.0 for removal of U(VI) ions on both adsorbents indicate positive cooperativity in binding and heterogeneous nature of adsorption (Table 2).

Effect of temperature and the thermodynamic parameters

The effect of temperature on the adsorption of U(VI) ions was realized at three different temperatures (Table 2). There was an increase in the adsorption capacities of both the fungal preparations as the temperature increases from 288 to

Table 2 Langmuir and Freundlich isotherm model constants and correlation coefficients determined in the adsorption process of U(VI) ions to native and DABSA-modified fungal biomass

Adsorbent	T (K)	Langmuir constant				Freundlich constant			
		$q_{e,\,exp}$ (mg/g)	q_m (mg/g)	$b \times 10^{-4}$ (L/mol)	R^2	R_L*	n	K_F	R^2
Native Fungal Biomass	288	99.2	121.0	0.247	0.987	0.140	1.92	5.19	0.912
	298	118.6	138.5	0.334	0.989	0.108	2.07	8.06	0.884
	308	132.7	147.1	0.498	0.996	0.075	2.46	13.8	0.889
DABSA-Modified Fungal Biomass	288	486.9	515.6	1.26	0.997	0.029	2.52	66.70	0.891
	298	539.2	549.5	4.60	0.999	0.008	5.07	181.9	0.714
	308	583.7	584.4	10.1	0.998	0.004	5.61	234.4	0.783

*C_0 = 500 mg/L

308 K for all U(VI) ions signifying that the adsorption was endothermic in nature. This could be due to the increasing number of binding sites that may have generated by expanding of pore mounts, and also increase in collision efficiency among the adsorbent and U(VI) ions in the bulk. Since the influences of energy consumption and adsorption capacity, the temperature of 298 K was selected as the optimum temperature for the removal of uranyl ions by the fungal biomass preparations.

The Gibbs free energy change (ΔG°) of adsorption process was calculated by using the following equations:

$$\Delta G = -RT \ln K_a \quad (4)$$

where K_a (L/mol) is the dependency of the equilibrium association constant ($K_a = b$, from Langmuir constant). R and T are the universal gas constant (8.314 J/K/mol) and solution temperature (K), respectively.

Standard enthalpy (ΔH) and entropy change (ΔS) values of adsorption can be calculated from van't Hoff equation given as:

$$\ln K_a = -\Delta H/RT + \Delta S/R \quad (5)$$

The K_a or b (L/mol) was used in the van't Hoff equation, in order to estimate the thermodynamic parameters [19, 51].

The values of ΔG, ΔH, and ΔS were calculated and presented in Table 2. The negative values of ΔG suggested that the adsorption of U(VI) ions on the fungal biomass preparations were spontaneous (Table 3). The ΔG values were amplified with the increasing of the solution temperature and displayed that the adsorption process was more reasonable at higher temperatures for the both adsorbents. In general, the ΔG values for physical, combined physical/chemical, and chemical adsorption are in the range of 0 to − 20 kJ mol^{-1}, − 20 to − 80 kJ/mol, and − 80 to − 400 kJ/mol, respectively [28]. In the presented study, as given in Table 2, the ΔG values were found to be in the range –18.7 and –21.8 kJ/mol and − 22.6 and − 29.5 kJ/mol for the native and DAPSA ligand attached fungal biomasses. These results illuminated that the adsorption process for both tested adsorbents was spontaneous physical and chemical adsorption functioned together. The positive values of ΔS indicated that the U(VI) ions had high affinity to the tested adsorbents which could be described the increasing randomness at medium/sorbent boundary during adsorption. The positive value of ΔH° (25.9 for the native and 77.3 kJ mol^{-1} for the DAPSA ligand attached) proposed that the adsorption process of U(VI) on the adsorbents were endothermic and spontaneous (Table 3).

Effect of contact time and evaluation of adsorption kinetics

The effect of contact time on U(VI) adsorption of the native and DAPSA ligand attached fungal biomass preparation is presented in Fig. 9. As observed from the figure, the adsorption capacity of the DAPSA ligand attached fungal biomass was rapidly increased and reached the equilibrium adsorption time within the first 20 min, whereas the adsorption capacity of the native fungal biomass was slowly increased and reached equilibrium about within 40 min. The certain strong-ion exchange properties of the DAPSA ligand attached fungal biomass may be the key explanations for the high adsorption rate. To evaluate the mechanism of the adsorption process, the experimental results were analyzed using pseudo-first-order and second order kinetic models. The kinetic models can be described by the following equations:

$$\log\left(q_{eq} - q_t\right) = \log q_{eq} - \left(k_1 \cdot t\right)/2.303 \quad (6)$$

$$\left(t/q_t\right) = \left(1/k_2 q_{eq}^2\right) + \left(1/q_{eq}\right)t \quad (7)$$

The kinetic parameters of the tested models are presented in Table 4. Compared with the first-order kinetic models, the value of R^2 was found to be very high (0.997–0.999) for the pseudo-second-order kinetic. Additionally, the calculated adsorption capacities were also very near to the experimental adsorption capacities of the tested adsorbents. As observed from Fig. 9, the second order model fitted best the experimental data. In addition, the calculated experimental adsorption capacities of the native and DAPSA ligand attached fungal biomasses were found to be 118.6 and 539.2 mg/g, and the theoretical adsorption capacities were obtained from the

Table 3 Thermodynamic parameters for adsorption of U(VI) ions to native and DABSA-modified fungal biomass

Adsorbent	T (K)	ΔG (kJ/mol)	ΔS (kJ/mol)	ΔH (kJ/mol K)	E_a (kJ/mol)
Native Fungal Biomass	288	−18.7	0.156	25.9	−9.25
	298	−20.1			
	308	−21.8			
DABSA-Modified Fungal Biomass	288	−22.6	0.349	77.3	−16.3
	298	−26.6			
	308	−29.5			

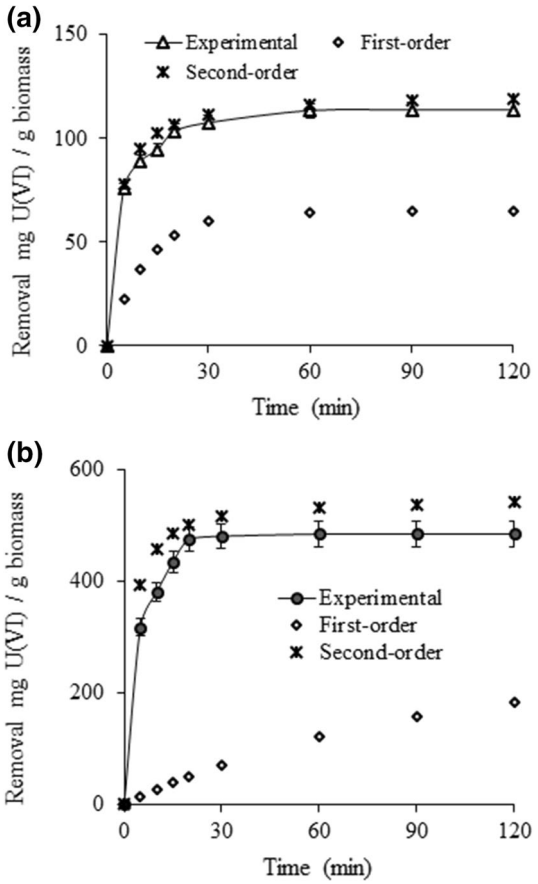

Fig. 9 Effect of contact time on adsorption of U(VI) ions on the native and DABSA modified fungal biomass preparations. Conditions: adsorbent dose, 0.4 g/L; U(VI) concentration, 200 mg/L; temperature, 25 °C; medium pH, 6.0 for the native and 5.0 for DABSA modified fungal biomass preparations; time, 2.0 h; stirring rate, 150 rpm)

pseudo-second-order equations were close to the experiment adsorption capacities (121.9 and 550.9 mg/g, respectively). These results showed that the adsorption of U(VI) ions on the tested adsorbents follow the pseudo-second-order model, which proposed that the rate-controlling step of the uranium removal process could be physical adsorption.

Effect of co-existing cations

In natural water sources, several metals ions are present, therefore, the effect of existing other cations in medium, such as Na(I), K(I), Ca(II), Ba(II), Cu(II) and Fe(II), on U(VI) ions adsorption capacities of tested was also examined. The concentration of these ions in each binary mixture was 50 mmol/L. The experimental data are presented in Fig. 10, as can be seen from the figure, the U(VI) adsorption capacity of the DAPSA ligand attached fungal biomass preparations were not significantly changed in the presence of Na(I), and K(I), ions in the adsorption medium. Whereas the presence of Ba(II), Ca(II), Cu(II), and Fe(II) in the adsorption medium, the adsorption capacity of the adsorbent was reduced. As observed from Fig. 10, Cu(II) and Fe(II) ions were expressively reduced U(VI) adsorption capacity of the adsorbent, and these metals ions intensely competed with the binding sites of U(VI) ions [50]. As reported earlier, strong cation-exchange adsorbent shows high affinity to metal ions with high valance charge and the adsorption is determined mostly by the valence of the metal cation [51]. When the metal cations with the same charge, the affinity of the strong-cation exchange adsorbent is towards the cation with the bigger ionic radii [50, 51]. As stated above, the obtained results are supported by the literature.

Desorption and reusability

For practical applications, the investigation of the reusability and desorption efficiency is essential. Therefore, the U(VI) laden fungal biomass preparations were subjected to desorption process to regenerate adsorbents with elution agent. Low concentration of HNO_3 (i.e., 20 mmol/L HNO_3) was found to be a highest desorption rate for both native and DAPSA modified fungal biomass preparations (Fig. 11, partly A and B, respectively). Thus, it was selected as the eluent for the regeneration of U(VI) laden fungal biomass preparations. The regenerated adsorbents were reused for adsorption U(VI). The fungal biomass preparations were washed with phosphate buffer solution (20 mmol/L, pH

Table 4 First and second order kinetic parameters for the adsorption of U(VI) ions to native and DABSA-modified fungal biomass

Adsorbent	T (K)	First-order				Second-order			
		q_{exp} (mg/g)	q_{eq} (mg/g)	$k_1 \times 10^2$ (min^{-1})	R^2	q_{eq} (mg/g)	$k_2 \times 10^3$ (g/mg/min)	R^2	h (mg/g min)
Native Fungal Biomass	288	99.2	30.7	6.69	0.953	102.3	3.43	0.999	35.9
	298	118.6	65.0	8.48	0.999	121.9	2.91	0.999	43.2
	308	132.7	79.4	9.54	0.989	136.8	2.67	0.998	49.9
DABSA-Modified Fungal Biomass	288	486.9	303.8	1.17	0.973	497.3	1.01	0.997	249.7
	298	539.2	244.6	1.14	0.991	550.9	0.91	0.998	276.2
	308	583.7	407.3	1.32	0.997	598.8	0.65	0.999	233.0

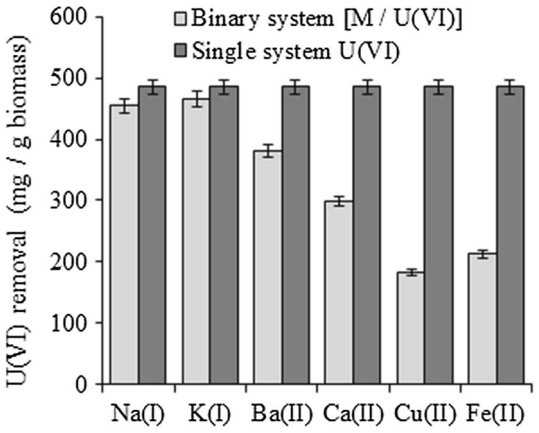

Fig. 10 Effect of co-existing other cation on U(VI) adsorption performance of the DABSA modified fungal biomass

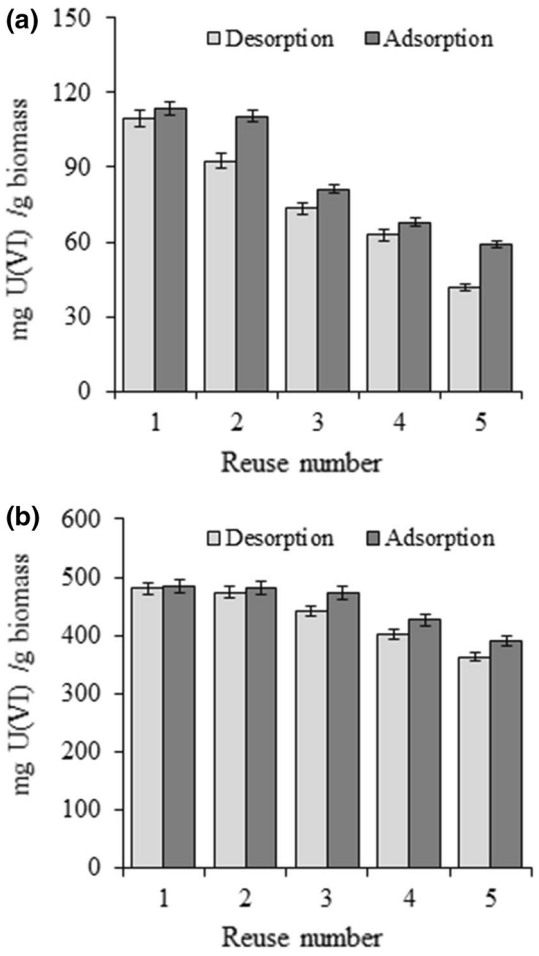

Fig. 11 The reusability and desorption efficiency of the native (**A**) and DABSA modified fungal biomass (**B**) preparation for adsorption–desorption cycles of U(VI) ions

6.5), and dried under reduced pressure at 45 °C for 6.0 h for the reuse in the subsequent adsorption–desorption cycle. The adsorption and desorption experiments were repeated five times by using the same fungal biomass preparations. As presented in Fig. 11 (partly A and B), after 5 repeated use, the adsorption capacities of native and DAPSA ligand attached fungal biomasses were still 11.9 and 77.9% of their initial adsorption capacities, respectively. These high regeneration capability of the fungal biomass preparations showed that they could be used as economic and environmentally friendly adsorbents for removing radionuclides from aqueous solutions.

The comparison of adsorption capacities of selected sorbents

For the purpose of the predictions of possible applications, the efficacy of the 2,5-diaminobenzenesulfonic acid ligand modified biomass of *Lentinus concinnus* was compared with the other modified sorbents in Table 5, the adsorption capacity of modified fungal biomass is comparable to that of the reported studied [52–58]. The results confirmed that the 2,5-diaminobenzenesulfonic acid ligand modified fungal biomass had a great potential for large scale applications.

Conclusion

Lentinus concinnus biomass was effectively utilized after modification with DABSA ligand. As prepared adsorbent is an environmental friendly and also has high adsorption capacity for U(VI) ions. The removal of uranyl ions was examined under different experimental conditions and the maximum U(VI) adsorption values were found to be 35 ◦C and about pH 6.0 for native fungal biomass, and about 5.0 for DAPSA ligand attached counterpart. The contact time studies presented that equilibrium adsorption of U(VI) ions was realized within 20 min for DABSA ligand attached fungal biomass. The maximum adsorption capacities of the native and DABSA ligand attached fungal biomasses were found to be 118.3 and 539.2 mg/g, respectively. The experimental adsorption equilibrium data was defined by the Langmuir model with high R^2 values. The pseudo-second order model was appropriate to describe the adsorption kinetic of the native and DABSA functionalized biomasses. FTIR and zeta-sizer analysis established that large quantity of primary and secondary amine, hydroxyl, carboxyl and sulfate groups were accountable functional groups for adsorption of U(VI) ions on both the tested fungal biomasses. Among above functional groups, the amine and sulfate groups could be most important for adsorption of U(VI) from aqueous medium. The adsorption capacity of the DABSA functionalized fungal biomass

Table 5 The comparison of adsorption capacities of selected sorbents

Adsorbents Native/modified	Initial U(VI) concentration (mg/L)	Adsorption capacity (mg/g) Native/Modified	References
Chitosan-chitosan-PO_4	50	162.5/384.6	[6]
Polymer-NH_2/Amidoxime	600	86.2/760.3	[11]
Bangia atropurpurea/nitrilotriacetate	300	190.2/328.8	[18]
Sugar beet pulp (SBP) /SBP-chemically modified	60	19.8/20.5	[41]
Trametes trogii/amidoxime	1000	238.2/447.4	[53]
Orange peel/amidoxime	300.0	155.4/382.9	[54]
Marine fungus/tri-amidoxime	40	15.46/584.6	[55]
Magnetic chitosan/amidoxime	44.5	– /357.0	[56]
Grapheneoxide (GO)/GO-diethylenetriaminepentaacetic phenylenediamine	50	97.3/485.0	[57]
Amidoxime modified calix[6]arene derivative with A. niger-Fe_3O_4	10	– /74.0	[58]
Sun flower straw	20	– /6.9	[59]
Lentinus concinnus/2,5-diaminobenzenesulfonic acid ligand	500	118.6/539.2	In this work

was widely increased compared to native biomass due to the presence strong interaction of primary amino and sulfate groups with U(VI) ions [45, 46]. Finally, the U(VI) adsorption process on both the fungal biomass preparations was spontaneous and increased randomness. Furthermore, the DAPSA ligand attached fungal biomass showed a high adsorption capacity with an excellent reusability, and it could be a good candidate for removal of metals from solution.

Acknowledgements The authors on behalf of National Institute of Agrobiological Sciences (NIAS) wish to offer many thanks for supplying the white rot fungus (*Lentinus concinnus*).

Author contributions The manuscript was written through contributions of all authors. All authors have given approval to the final version of the manuscript.**CRediT authorship contribution statement** Omur Celikbical: Methodology, Investigation, Formal analysis. Gulay Bayramoglu: Conceptualization, Methodology, Investigation, Validation, Writing—original draft, Funding acquisition. Ilkay Acıkgoz-Erkaya: Methodology, Visualization, Investigation. Mehmet Yakup Arica: Project administration, Supervision, Writing—review & editing.

Declaration

Competing of interest The authors declare that they have no known competing financial interests or personal relationships that could have appeared to influence the work reported in this paper.

References

1. Zhu W, Liu Z, Chen L, Dong Y (2011) Sorption of uranium(VI) on Na-attapulgite as a function of contact time, solid content, pH, ionic strength, temperature and humic acid. J Radioanal Nucl Chem 289(3):781–788
2. Liang L, Lin X, Liu Y, Sun S, Chu H, Chen Y, Liu D, Luo X, Zhang J, Shang R (2020) Carboxymethyl konjac glucomannan mechanically reinforcing gellan gum microspheres for uranium removal. Inter J Biol Macromol 145:535–546
3. Ozturk M, Zorer OS, Gulcan M (2021) Synthesis and characterization of UTSA-76 metal organic framework containing Lewis basic sites for the liquid-phase adsorption of U(VI). Colloid Surf A 609:125663
4. Kolhe N, Zinjarde S, Acharya C (2020) Removal of uranium by immobilized biomass of a tropical marine yeast *Yarrowia lipolytica*. J Environ Radioact 223–224:106419
5. Zhou Y, Li Y, Liu D, Wang X, Liu D, Xu L (2020) Synthesis of the inorganic-organic hybrid of two-dimensional polydopamine-functionalized titanate nano-sheets and its efficient extraction of U(VI) from aqueous solution. Colloid Surf A 607:125422
6. Sun Y, Kang Y, Zhong W, Liu Y, Dai Y (2020) A simple phosphorylation modification of hydrothermally cross-linked chitosan for selective and efficient removal of U(VI). J Solid State Chem 292:121731
7. Tuzen M, Saleh TA, Sarı A, Naeemullah (2020) Interfacial polymerization of trimesoyl chloridewith melamine and palygorskite for efficient uranium ions ultra-removal. Chem Eng Res Des 159:353–361
8. Bai Z, Liu Q, Song D, Zhang H, Liu J, Chen R, Yu J, Li R, Wang J (2020) Preparation of a 3D multi-branched chelate adsorbent for high selective adsorption of uranium(VI): Acrylic and diaminomaleonitrile functionalized waste hemp fiber. React Funct Polym 149:104512
9. Tang N, Liang J, Niu C, Wang H, Luo Y, Xing W, Ye S, Liang C, Guo H, Guo J, Zhang Y, Zeng G (2020) Amidoxime-based materials for uranium recovery and removal. J Mater Chem A 8:7588

10. Mohammed AAR (2020) Potentiality of quercetin-sodium hydroxide modified *SpirulinaPlatensis* in uranium biosorption from waste effluent. Int J Environ Stud 77:48–60
11. Bayramoglu G, Arica MY (2019) Star type polymer grafted and polyamidoxime modified silica coated-magnetic particles for adsorption of U(VI) ions from solution. Chem Eng Res Des 147:146–159
12. Singhal P, Vats BG, Pulhani V (2020) Magnetic nanoparticles for the recovery of uranium from sea water: Challenges involved from research to development. J Ind Eng Chem 90:17–35
13. Bai J, Ma X, Yan H, Zhu J, Wang K, Wang J (2020) A novel functional porous organic polymer for removal of uranium from wastewater. Micropor Mesopor Mater 306:110441
14. Huang Y, Zheng H, Li H, Zhao C, Zhao R, Li S (2020) Highly selective uranium adsorption on 2-phosphonobutane-1,2,4-tricarboxylic acid-decorated chitosan-coated magnetic silica nanoparticles. Chem Eng J 388:124349
15. Puspitasari T, Darwis D, Pangerteni DS, Seftiani S, Nurhasni N (2020) Synthesis and characterization of zeolite–amo hybrid composite adsorbent by using simultaneous gamma irradiation for uranium (VI) removal from aqueous solutions. Macromol Symp 391:1900156
16. Chen L, Ning S, Huang Y, Chen Y, Ju Z, He X, Lu L, Zhou H, Wang X, Wu Y, Wei Y (2020) Effects of speciation on uranium removal efficiencies with polyamine functionalized silica composite adsorbent in groundwater. J Clean Produc 256:120379
17. Hamza MF, Mubark AE, Wei Y, Vincent T, Guibal E (2020) Quaternization of composite algal/PEI beads for enhanced uranium sorption—application to ore acidic leachate. Gels 6:12
18. Bayramoglu G, Akbulut A, Acıkgoz-Erkaya I, Arica MY (2018) Uranium sorption by native and nitrilotriacetate-modified Bangia atropurpurea biomass: kinetics and thermodynamics J Appl Phycol 30:649–661
19. Bayramoglu G, Arica MY (2017) Polyethylenimine and tris(2-aminoethyl)amine modified p(GMA-co-EGDMA) microbeads for adsorption of U(VI) ions: Equilibrium, kinetic and thermodynamic studies. J Radioanal Nucl Chem 312:293–303
20. Ahmad M, Wang J, Yang Z, Zhang Q, Zhang B (2020) Ultrasonic-assisted preparation of amidoxime functionalized silica framework via oil-water emulsion method for selective uranium adsorption. Chem Eng J 389:124441
21. Janu VC, Meena RK, Kumar N, Sharma RK (2020) Surface fluorinated hematite for uranium removal from radioactive effluent. J Environ Chem Eng 8:104218
22. Amesh P, Suneesh AS, Venkatesan KA, Chandra M, Ravindranath NA (2020) High capacity amidic succinic acid functionalized mesoporous silica for the adsorption of uranium. Colloid Surf A 602:125053
23. Boulanger N, Kuzenkova AS, Iakunkov A, Romanchuk AY, Trigub AL, Egorov AV, Bauters S, Amidani L, Retegan M, Kvashnina KO, Kalmykov SN, Talyzin AV (2020) Enhanced sorption of radionuclides by defect-rich graphene oxide. ACS Appl Mater Interfaces 12:45122–45135
24. Yousef LA, Bakry AR, Abd El-Magied MO (2020) Uranium (VI) recovery from its leach liquor using zirconium molybdophosphate composite: kinetic, equilibrium and thermodynamic studies. J Radioanal Nucl Chem 323:549–556
25. Khan A, Wei D, Khuda F, Ma R, Ismail M, Ai Y (2020) Comparative adsorption capabilities of rubbish tissue paper–derived carbon-doped MgO and CaCO3 for EBT and U(VI), studied by batch, spectroscopy and DFT calculations. Environ Sci Pollut Res 27:13114–13130
26. Huo Z, Zhao S, Yi J, Zhang H, Li J (2020) Biomass-based cellulose functionalized by phosphonic acid with high selectivity and capacity for capturing U(VI) in aqueous aolution. Appl Sci 10:5455
27. Arica MY, Bayramoglu G (2016) Polyaniline coated magnetic carboxymethylcellulose beads for selective removal of uranium ions from aqueous solution. J Radioanal Nucl Chemy 310:711–724
28. Bayramoglu G, Arica MY (2016) Amidoxime functionalized Trametes trogii pellets for removal of uranium (VI) from aqueous medium. J Radioanal Nucl Chem 307:373–384
29. Hamza MF, Gamal A, Hussein G, Ngar MS, Abdel-Rahman AA-H, Wei Y, Guibal E (2019) Uranium(VI) and zirconium(IV) sorption on magnetic chitosan derivatives – effect of different functional groups on separation properties. J Chem Technol Biotechnol 94:3866–3882
30. Zhang W, Dong F, Liu M, Song H, Nie X, Huo T, Zhao Y, Wang P, Qin Y, Zhou L (2020) Reduction and enrichment of uranium after biosorption on inactivated *Saccharomyces cerevisiae*. Pol J Environ Stud 29:1461–1472
31. Bayramoglu G, Arica MY (2016) MCM-41 silica particles grafted with polyacrylonitrile: Modification in to amidoxime and carboxyl groups for enhanced uranium removal from aqueous medium. Micropor Mesopor Mater 226:117–124
32. Bayramoglu G, Akbulut A, Arica MY (2015) Study of polyethyleneimine and amidoxime functionalized hybrid biomass of Spirulina (Arthrospira) platensis for adsorption of uranium (VI) ion. Environ Sci Pollut Res 22:17998–18010
33. Yousef LA, Bakry AR, Ahmad AA (2020) Uranium(VI) recovery from acidic leach liquor using manganese oxidecoated zeolite (MOCZ) modified with amine. J Radioanal Nucl Chem 324:409–421
34. Chaudharya M, Singhb L, Rekhac P, Srivastavab VC, Mohanty P (2019) Adsorption of uranium from aqueous solution as well as seawater conditions by nitrogen-enriched nanoporous polytriazine. Chem Eng J 378:122236
35. Yousef LA, Bakry AR, Ahmad AA (2020) Uranium(VI) adsorption using a mixture of 1-amino-2-naphthol-4-sulfonic acid and bentonite: kinetic and equilibrium studies. Radiochemistry 62:511–523
36. Bayramoglu G, Yilmaz M (2018) Azo dye removal using free and immobilized fungal biomasses: isotherms, kinetics and thermodynamic studies. Fibers and Polymers 19:877–886
37. Perez-Bustamante JA, Delgado FP (1971) The extraction and spectrophotometric determination of sexavalent uranium with arsenazo11 in aqueous-organic media. Analyst 96:407422
38. Bayramoglu G, Arica MY (2021) Strong and weak cation-exchange groups generated cryogels films for adsorption and purification of lysozyme. Food Chem 342:128295
39. Fang C, Tao Q, Dai Y (2020) Amidoximated orange peel as a specific uranium scavenger. J Radioanal Nucl Chem 326:1831–1841
40. Al-Anber MA, Al-Momani IF, Zaitoun MA, Al-Qaisi W (2020) Inorganic silica gel functionalized tris(2-aminoethyl)amine moiety for capturing aqueous uranium (VI) ion. J Radioanal Nucl Chem 325:605–623
41. Nuhanovic M, Grebo M, Draganovic S, Memic M, Smjecanin N (2019) Uranium(VI) biosorption by sugar beet pulp: equilibrium, kinetic and thermodynamic studies. J Radioanal Nucl Chem 322:2065–2078
42. Sabanovic E, Muhic-Sarac T, Nuhanovic M, Memic M (2019) Biosorption of uranium (VI) from aqueous solution by Citrus limon peels: kinetics, equilibrium and batch studies. J Radioanal Nucl Chem 319:425–435
43. Hamza MF, Wei Y, Benettayeb A, Wang X, Guibal E (2020) efficient removal of uranium, cadmium and mercury from aqueous solutions using grafted hydrazide-micromagnetite chitosan derivative. J Mater Sci 55:4193–4212
44. Liu L, Lin X, Li M, Chu H, Wang H, Xie Y, Du Z, Liu M, Liang L, Gong H, Zhou J, Li Z, Luo X (2021) Microwave-assisted hydrothermal synthesis of carbon doped with phosphorus for uranium(VI) adsorption. J Radioanal Nucl Chem 327:73–89

45. Ang KL, Li D, Nikoloski AN (2017) The effectiveness of ion exchange resins in separating uranium and thorium from rare earth elements in acidic aqueous sulfate media. Part 1. Anionic and cationic resins Hydrometallurgy 174:147–155
46. Wang J, Yang S, Cheng G, Gu P (2020) The adsorption of europium and uranium on the sodium dodecyl sulfate modified molybdenum disulfide composites. J Chem Eng Data 65:2178–2185
47. Arica TA, Ayas E, Arica MY (2017) Magnetic MCM-41 silica particles grafted with poly (glycidylmethacrylate) brush: Modification and application for removal of direct dyes. Micropor Mesopor Mater 243:64–175
48. Dolatyari L, Shateri M, Yaftian MR, Rostamnia S (2019) Unmodified SBA-15 adsorbents for the removal and separation of Th(IV) and U(VI) ions: the role of pore channels and surface-active sites. Sep Sci Technol 54:2863–2878
49. Gado M, Atia B, Morcy A (2019) The role of graphene oxide anchored 1-amino-2-naphthol-4-sulphonic acid on the adsorption of uranyl ions from aqueous solution: kinetic and thermodynamic features. Int J EnvironAnal Chem 99:996–1015
50. Gao Z, Bandosz TJ, Zhao Z, Han M, Qiu J (2009) Investigation of factors affecting adsorption of transition metals on oxidized carbon nanotubes. J Hazard Mater 167:357–365
51. Lima EC, Hosseini-Bandegharaei A, Moreno-Piraján JC, Anastopoulos IA (2019) Critical review of the estimation of the thermodynamic parameters on adsorption equilibria. Wrong use of equilibrium constant in the Van't Hoof equation for calculation of thermodynamic parameters of adsorption. J Mol Liq 273:425–434
52. Escudero C, Poch J, Villaescusa I (2013) Modelling of breakthrough curves of single and binary mixtures of Cu(II), Cd(II), Ni(II) and Pb(II) onto grape stalks waste. Chem Eng J 1217:129–138
53. Bayramoglu G, Arica MY (2016) Amidoxime functionalized *Trametes trogii* pellets for removal of uranium(VI) from aqueous medium. J Radioanal Nucl Chem 307:373–384
54. Fang C, Tao Q, Dai Y (2020) Amidoximated orange peel as a specifc uranium scavenger. J Radioanal Nucl Chem 326:1831–1841
55. Han J, Hu L, He L, Ji K, Liu Y, Chen C, Luo X, Tan N (2020) Preparation and uranium (VI) biosorption for tri-amidoxime modified marine fungus material. Environ Sci Pollut Res 27:37313–37323
56. Hamza MF, Roux JC, Guibal E (2018) Uranium and europium sorption on amidoxime-functionalized magnetic chitosan microparticles. Chem Eng J 344:124–137
57. Liu S, Ouyang J, Luo J, Sun L, Huang G, Ma J (2018) Removal of uranium(VI) from aqueous solution using graphene oxide functionalized with diethylenetriamine pentaacetic phenylenediamine. J Nucl Sci Technol 55:781–791
58. Li L, Tang S, Cheng B, Liao Q, Lu W, Dai Z, Tan Y, Sun J (2018) Synthesis and adsorption characteristics of calix[6]arene derivative modified Aspergillus niger-Fe_3O_4 bio-nanocomposite for U(VI). J Radioanal Nucl Chem 316:331–339
59. Ai L, Luo X, Lin X, Zhang S (2013) Biosorption behaviors of uranium (VI) from aqueous solution by sunflower straw and insights of binding mechanism. J Radioanal Nucl Chem 298:1823–1834